

Small gases adsorption and related reactions on CeO₂ nanoparticle

Mr. Pattanarak Swing

ภาควิชาเคมี
คณะวิทยาศาสตร์
จุฬาลงกรณ์มหาวิทยาลัย

In Partial Fulfillment for the Degree of Bachelor of Science

Department of Chemistry, Faculty of Science

Chulalongkorn University

Academic Year 2014

การศึกษาการดูดซับก๊าซและปฏิกิริยาที่เกิดขึ้นบนอนุภาคนาโนซีเรีย



นายพัฒนรักษ์ สวิง

ภาควิชาเคมี
คณะวิทยาศาสตร์
จุฬาลงกรณ์มหาวิทยาลัย

โครงการนี้เป็นส่วนหนึ่งของการศึกษาตามหลักสูตรปริญญาวิทยาศาสตรบัณฑิต

ภาควิชาเคมี คณะวิทยาศาสตร์

จุฬาลงกรณ์มหาวิทยาลัย

ปีการศึกษา 2557

Small gases adsorption and related reactions on CeO₂ nanoparticle

Mr. Pattanarak Swing

ภาควิชาเคมี
คณะวิทยาศาสตร์
จุฬาลงกรณ์มหาวิทยาลัย

In Partial Fulfillment for the Degree of Bachelor of Science

Department of Chemistry, Faculty of Science

Chulalongkorn University


Academic Year 2014

Project Title: Small gases adsorption and related reactions on CeO₂ nanoparticle
By: Mr. Pattanarak Swing
Field of study: Chemistry
Project Advisor: Professor Vithaya Ruangpornvisuti, Dr.rer.nat

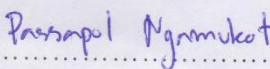
PROJECT COMMITTEE

..... Chair committee

(Associate Professor Viwat Vachirawongkawin, Dr.rer.nat.)

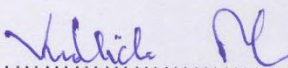
..... Project Advisor

(Professor Vithaya Ruangpornvisuti, Dr.rer.nat.)

..... Committee

(Dr. Passapol Ngamukot, Ph.D.)

Accepted by Department of Chemistry, Faculty of Science, Chulalongkorn University in
Partial Fulfillment of the Requirements for the Degree of Bachelor of Science.

..... Head of Department of Chemistry

(Associate Professor Vudhichai Parasuk, Ph.D.)

14 / July / 2015

Writing quality of this report is : Very good Good Pass

ชื่อโครงการ การศึกษาการดูดซับก๊าซและปฏิกิริยาที่เกิดขึ้นบนอนุภาคนาโนซีเรีย

ชื่อนิติในโครงการ นายพัฒนรักษ์ สวีง เลขประจำตัว 5433123823

ชื่ออาจารย์ที่ปรึกษา ศ.ดร.วิทยา เรื่องพรวิสุทธิ

ภาควิชา เคมี คณะวิทยาศาสตร์ จุฬาลงกรณ์มหาวิทยาลัย ปีการศึกษา 2557

บทคัดย่อ

ศึกษาการดูดซับโมเลกุลก๊าซได้แก่ ไฮโดรเจน, ไนโตรเจน, ออกซิเจน, คาร์บอนมอนอกไซด์, ไนโตรเจนมอนอกไซด์, คาร์บอนไดออกไซด์, ไดไนโตรเจนมอนอกไซด์, ไนโตรเจนไดออกไซด์, น้ำ, ไดไฮโดรเจนซัลไฟด์, ซัลเฟอร์ไดออกไซด์, อีโพรน, อีทีน, มีเทน และแอมโมเนีย ที่ถูกดูดซับบนอนุภาคนาโนซีเรียได้แก่ ซีเรียมไดออกไซด์ (CeO_2) และไดซีเรียมเตตระออกไซด์ (Ce_2O_4) โดยการคำนวณด้วยวิธี DFT/B3LYP/GEN พบว่าการดูดซับของน้ำบน CeO_2 และ Ce_2O_4 ดูดซับได้ดีที่สุด ซึ่งค่าการดูดซับบน CeO_2 และ Ce_2O_4 เป็น -51.45 และ -52.45 กิโลแคลอรีต่อโมล ตามลำดับ ค่าช่องว่างพลังงานของ CeO_2 และ Ce_2O_4 มีค่าลดลงมากหลังจากดูดซับโมเลกุลออกซิเจน และไนโตรเจนมอนอกไซด์ ดังนั้น CeO_2 และ Ce_2O_4 สามารถนำไปเป็นวัสดุรับรู้ก๊าซออกซิเจนและก๊าซไนโตรเจนมอนอกไซด์ได้ และยังพบว่าปฏิกิริยารีดักชันของ CeO_2 ไปเป็น CeO โดยก๊าซไฮโดรเจนนั้นไม่สามารถเกิดขึ้นเองได้ที่อุณหภูมิ 298 เคลวิน ซึ่งค่าพลังงานอิสระมีค่า 234.1 กิโลแคลอรีต่อโมล

ภาควิชาเคมี
คณะวิทยาศาสตร์
จุฬาลงกรณ์มหาวิทยาลัย

ภาควิชา เคมีลายมือชื่อนิติ.....

สาขาวิชา เคมีลายมือชื่ออาจารย์ที่ปรึกษาโครงการ.....

ปีการศึกษา 2557

Project Title: Small gases adsorption and related reactions on CeO₂ nanoparticle

Student name: Mr. Pattanarak Swing **Student ID:** 5433123823

Advisor: Professor Vithaya Ruangpornvisuti, Dr.rer.nat.

Department of Chemistry, Faculty of Science, Chulalongkorn University, Academic Year 2014

ABSTRACT

Adsorptions of diatomic (H₂, N₂, O₂, CO, NO), triatomic (CO₂, N₂O, NO₂, H₂O, H₂S, SO₂) and polyatomic (C₂H₂, C₂H₄, CH₄, NH₃) gases on CeO₂ and Ce₂O₄ clusters were studied using the DFT/B3LYP/GEN method. Water adsorptions on Ce atom of CeO₂ and Ce₂O₄ clusters were found to be the most favorable process. The adsorption enthalpies for water adsorbed on the CeO₂ and Ce₂O₄ clusters are -51.45 and -52.45 kcal/mol, respectively. Energy gaps of CeO₂ and Ce₂O₄ clusters largely decreased after adsorptions of O₂ and NO gases. The CeO₂ and Ce₂O₄ clusters can therefore be used as the sensing materials for O₂ and NO detections. It was found that the CeO₂ reduced to the CeO cluster by H₂ gas is non-spontaneous reaction at 298 K; the Gibbs free energy of the reaction is 234.1 kcal/mol.



Department: Chemistry Student's Signature

Field of Study: Chemistry Advisor's Signature

Academic Year 2014

ACKNOWLEDGEMENTS

I would like to gratefully thank my advisor Prof. Dr. Vithaya Ruangpornvisuti for his very useful guidance and encouragement during the course of this project. Without his instruction and guidance, the project could not be completed. He provided an opportunity for me to be able to join the project under his instruction with kindness and generous. I were very appreciating of your guidance and patience during the time. When I were spending in laboratory. Also I have appreciated my seniors, who encouraged and gave me tips to get the work done. I will not get this far without their helps. I would like to give special thank to my committee: Assoc. Prof. Viwat Vachirawongkawin and Dr. Passapol Ngamukot who are giving me the instruction and advice on how to write the complete project report.

Mr. Pattanarak Swing



ภาควิชาเคมี
คณะวิทยาศาสตร์
จุฬาลงกรณ์มหาวิทยาลัย

CONTENTS

	Page
ABSTRACT IN THAI.....	IV
ABSTRACT IN ENGLISH.....	V
ACKNOWLEDGEMENTS.....	VI
CONTENTS.....	VII
LIST OF FIGURES.....	IX
LIST OF TABLES.....	X
CHAPTER	
I. INTRODUCTION.....	1
1.1 Background and literature reviews.....	1
1.2 Theoretical background	2
1.2.1 Quantum chemical calculations.....	2
1.2.2 DFT method.....	3
1.2.2.1 The Kohn-Sham formalism.....	3
1.2.2.2 Hybrid methods.....	5
1.2.3 Gaussian basis sets.....	5
1.2.3.1 Minimal basis sets.....	6
1.2.3.2 Split-valence basis sets.....	6
1.2.3.3 Polarized functions.....	7
1.2.3.4 Effective core potentials.....	7
1.2.4 Chemical indices.....	7
1.2.4.1 Electronic chemical potential.....	7
1.2.4.2 Mulliken electronegativity.....	8
1.2.4.3 Chemical hardness.....	8
1.2.4.4 Electrophilicity.....	9
1.2.4.5 Dipole moment.....	9
1.2.5 Thermodynamic properties.....	9
1.2.5.1 Enthalpies and Gibbs free energies of reaction.....	9

1.2.5.2	Rate of reaction.....	11
1.3	Objective.....	11
II.	COMPUTATIONAL DETAILS.....	12
2.1	Computational methods.....	12
2.2	Definitions of reaction terms.....	12
2.2.1	Adsorption of small gases on ceria or cerium oxide...	12
2.2.2	Thermodynamic quantities.....	12
III.	RESULTS AND DISCUSSIONS.....	13
3.1	The optimized structures.....	13
3.2	Adsorption of single molecule of gases on the CeO ₂ and Ce ₂ O ₄ clusters.....	13
3.2.1	Adsorption of gases on the CeO ₂	13
3.2.2	Adsorption of gases on the Ce ₂ O ₄	18
3.3	The reduction of CeO ₂ to CeO by H ₂ gas.....	23
IV.	CONCLUSIONS.....	26
	REFERENCES.....	27
	VITAE.....	30



LIST OF FIGURES

Figure		Page
3.1	Figure 3.1 The B3LYP/GEN-optimized structures of (a) CeO ₂ and (b) trans-Ce ₂ O ₄	13
3.2	The adsorption configurations of (a) H ₂ , (b) N ₂ , (c) O ₂ , (d) CO (its C-end toward), (e) CO (its O-end toward), (f) NO (its N-end toward), (g) NO (its O-end toward), (h) CO ₂ , (i) N ₂ O (its N-end toward), (j) N ₂ O (its O-end toward), (k) NO ₂ , (l) H ₂ O, (m) H ₂ S, (n) SO ₂ , (o) C ₂ H ₂ , (p) C ₂ H ₄ , (q) CH ₄ , (r) NH ₃ on CeO ₂ cluster, computed at the B3LYP/GEN method. Their bond distances are in Å.....	15
3.3	The adsorption configurations of (a) H ₂ , (b) N ₂ , (c) O ₂ , (d) CO (its C-end toward), (e) CO (its O-end toward), (f) NO (its N-end toward), (g) NO (its O-end toward), (h) CO ₂ , (i) N ₂ O (its N-end toward), (j) N ₂ O (its O-end toward), (k) NO ₂ , (l) H ₂ O, (m) H ₂ S, (n) SO ₂ , (o) C ₂ H ₂ , (p) C ₂ H ₄ , (q) CH ₄ , (r) NH ₃ on Ce ₂ O ₄ cluster, computed at the B3LYP/GEN method. Their bond distances are in Å.....	20
3.4	B3LYP/GEN-optimized structures of CeO ₂ , CeO and the related intermediates and transition states.....	24
3.5	Potential energy profile for reduction of CeO ₂ to CeO by hydrogen gas....	25

LIST OF TABLES

Table		Page
3.1	Energy gap and chemical indices of CeO ₂ cluster and its gas adsorptions, computed at the DFT/B3LYP/GEN method.....	16
3.2	Adsorption energies of diatomic, triatomic and polyatomic gases on the CeO ₂ cluster, computed at the B3LYP/GEN method.....	17
3.3	Energy gap and chemical indices of Ce ₂ O ₄ cluster and its gas adsorption on the Ce ₂ O ₄ cluster, computed at the DFT/B3LYP/GEN method.....	21
3.4	Adsorption energies of diatomic, triatomic and polyatomic gases on the CeO ₂ cluster, computed at the B3LYP/GEN method.....	22
3.5	Energetics, thermodynamic properties, rate constants, and equilibrium constants of reduction reaction of CeO ₂ to CeO, computed at the DFT/B3LYP/GEN method.....	25



CHAPTER I

INTRODUCTION

1.1 Background and literature review

In petrochemical industry, Ceria or Ceriumdioxide (CeO_2) is popularly used because of many specific chemical characteristics. For example: UV-visible adsorption capability [1], high level of heat stabilization [2], electrolyte and diffusion [3], solid, specific chemical reaction [4], oxygen storage and oxygen transmittance capability [5]. Therefore, nanoceriumdioxide particle is one of the significant substances in the industry of petrochemical. This substance is used as a catalyst in some kinds of reaction such as hydrocarbon transformation, changing CO and NO_x into H_2O , CO_2 and N_2 in vehical system [6-10], solar cell, fuel cell, phosphorescent, luminescent, sensor gas etc. [11-14]. The information from the research of gas adsorption and ceriumdioxide surfaced reaction is a good source for estimating the reaction of ceriumdioxide surface. The special character on the surface consists of two features: crystal and nanoparticle.

In the year of 2009, Chen H. et al [15] analyzed the electronic properties of nanoparticle through the density functional theory. Fire algorithm binding with simulation of annealing process obtains all structures with global minimal energies and then DMOL3 program further re-optimized with double numerical atomic basis sets. Two helpful investigating methods are computed to describe the chemical reaction of different sites for nanoparticle.

In the year of 2010, Syzgantseva O. et al [16] analyzed the interaction between ZrO_2 molecule and H_2 within the DFT and CCSD approached. H_2 is firstly activated and then the cleavage of H-H bond effecting OZrH-OH species with hydride and hydroxyl groups. Both direct transfer and two step process via Zr intermediate leads to the formation of water generating ZrO into H_2O . The hybrid B3LYP or PBE0 functional with SDD basis set on Zr and 6-311 basis sets for O and H, representing the cooperation between accuracy and computational cost.

1.2 Theoretical background

Quantum Chemistry is categorized into semi-empirical, Hartree-Fock (HF) and density functional theory (DFT) methods to describe the behaviors of molecules. Quantum chemical studies relate to the ground state of individual atoms and molecules, to excited states, and to the transition states that occur throughout chemical reaction.

1.2.1 Quantum chemical calculations

According to quantum mechanics research (QM), this study describes a unit that quantum theory allocates into certain physical quantities; for example, the energy of an atom at ground state. The synopsis of QM were introduced by Max Planck, Niels Bohr, Louise de Broglie, Erwin Schrödinger, Werner Heisenberg and others. The significant features of hypothesis of QM is called wave function, exist for any chemical system, and that appropriate function which react upon Ψ return the noticeable properties of the system. The equivalent formulation of QM was invented by Schrödinger [17-21],

$$\hat{H}\Psi = E\Psi, \quad (1.1)$$

where \hat{H} is Hamiltonian operator, E is the total energy of the system and Ψ is the n-electron wave function, respectively.

The kinetic and potential energies within each molecule were indicated by the \hat{H} as illustrated in the equation. (1.2)

$$\hat{H} = -\frac{\hbar^2}{2m_e} \sum_i^{\text{electrons}} \nabla_i^2 - \frac{\hbar^2}{2} \sum_A^{\text{nuclei}} \frac{1}{M_A} \nabla_A^2 - \frac{e^2}{4\epsilon_0} \sum_i^{\text{electron}} \sum_A^{\text{nuclei}} \frac{Z_A}{r_{iA}} + \frac{e^2}{4\epsilon_0} \sum_i^{\text{electrons}} \sum_j^{\text{electrons}} \frac{1}{r_{ij}} + \frac{e^2}{4\epsilon_0} \sum_A^{\text{nuclei}} \sum_B^{\text{nuclei}} \frac{Z_A Z_B}{R_{AB}} \quad (1.2)$$

where Z is the nuclear charge, M_A is the mass of electron, R_{AB} is the distance between nuclei A and B, r_{ij} is the distance between electrons i and j , r_{iA} is the distance between electron i and nucleus, and ϵ_0 is the permittivity of vacuum.

1.2.2 DFT method

The idea of DFT [21-24] is the investigation of ground-state electronic energy by an electron density that was later confirmed by Hohenberg and Kohn in 1964. Therefore, this experiment is the pertinence between two factors: the electronic energy and electron density.

1.2.2.1 The Kohn-Sham formalism

The main problem of DFT concept is to describe how kinetic energy reacts in the system. The idea of kinetic energy function can be calculated into two terms; Firstly the electron itself was considered as non-interacting particles could be precisely estimated and secondly the energy function is a small correction term accounted for electron-electron interactions.

$$E[\rho] = -\frac{1}{2} \sum_{i=1}^n \int \Psi_i^*(r_1) \nabla_i^2 \Psi_i(r_1) dr_1 - \sum_{i=1}^N \int \frac{Z_i}{r_i} \rho(r_1) dr_1 + \frac{1}{2} \iint \frac{\rho(r_1) \rho(r_2)}{r_{12}} dr_1 dr_2 + E^C[\rho] \quad (1.3)$$

where Ψ_i ($i = 1, 2, 3, \dots, n$) are the Kohn-Sham orbitals, n is the number of electrons, N is the number of nuclei. The first term of the equation (1.3) accounts for the kinetic energy of the noninteracting electrons, the second term represents the nuclear-electron interactions, the third term known as the Coulombic repulsions between the total charge distributions and the fourth term corresponds to the exchange correlation which represents the correction of kinetic energy from the interacting repulsion between electron-electron.

As set of one-electron orbitals, the ground state electron density ($\rho(r)$) can be written as

$$\rho(r) = \sum_{i=1}^n |\Psi_i(r)|^2. \quad (1.4)$$

The Kohn-Sham orbitals are identified by solving the Kohn-Sham equations, given by

$$\hat{h}_i(\Psi_i)(r_1) = \varepsilon_i \Psi_i(r_1), \quad (1.5)$$

where ε_i is the Kohn-Sham orbital energy, and \hat{h}_i is the Kohn-Sham Hamiltonian, given by

$$\hat{h}_i = -\frac{1}{2} \nabla_1^2 - \sum_{i=1}^N \frac{Z_i}{r_{i1}} + \int \frac{\rho(r_2)}{r_{12}} dr_2 + E^C(r_1). \quad (1.6)$$

In equation (1.6) E^C is the functional derivative of the exchange-correlation energy that can be written as

$$E^C[\rho] = \frac{\delta E^C[\rho]}{\delta \rho}. \quad (1.7)$$

The exchange-correlation energy (E^C) is split into two terms that are shown in Equation (1.8)

$$E^C[\rho] = E^X[\rho] + E^C[\rho]. \quad (1.8)$$

The first term is exchange term (E^X) that generally associated with interactions between the same spin electrons and the second term is correlation term (E^C) that associated with interactions between opposite spin electrons.

1.2.2.2 Hybrid methods

The most widespread hybrid functional is referred from an exchange-energy functional invented by Becke and Steven that is the introduction of LYP correlation energy. Accordingly this correlation functional called B3LYP functional is as below.

$$E_{C}^{B3LYP} = (1-a_0-a_x) E_{C}^{LSDA} + a_0 E_{C}^{HF} + a_B E_{C}^B + (1-a_0) E_{C}^N + a_C E_{C}^{LYP}. \quad (1.9)$$

Here E_{C}^{LSDA} is the kind accurate pure DFT the local spin-density approximation (LSDA) non-gradient-corrected exchange functional, E_{C}^{HF} is the Kohn-Sham orbitals based HF exchange energy functional, E_{C}^B is the Becke 88 exchange functional

$$E_{C}^B = E_{C}^{LDA} + E_{C}^B; \quad (1.10)$$

$$E_{C}^B = -\frac{1}{3} \frac{x^2}{1+6|x|\sinh^{-1}x}.$$

The parameter is determined by fitting to known atomic data and x is a dimension gradient variable. The E_{C}^N is the Vosko, Wilk, Nusair function (VWN) is given by

$$E_{C}^N = E_{C}^{LDA} (1+ax^2+bx^4+cx^6)^{1/5}; \quad (1.11)$$

$$x = \left| \frac{\nabla}{4/3} \right|.$$

1.2.3 Gaussian basis sets

The basis sets are the mathematical function which used the DFT calculation to describe the electron allocation and model the shape of molecular orbitals and electron density [25]. These orbitals are estimated as linear combinations of the basic functions that

are named linear combination of atomic orbitals approach (LCAO). Nevertheless, the function was not popularly effective in terms of over-cost issue and early numerical calculations were forwarded using Slater-type orbitals (STOs).

$$(r, \theta, \phi) = \frac{(2\zeta/a_0)^{n+1/2}}{[(2n)!]^{1/2}} r^{n-1} e^{-\zeta r/a_0} Y_l^m(\theta, \phi). \quad (1.12)$$

Further work showed that the cost of calculations can be further reduced if the AOs are expanded in terms of Gaussian functions, which have the form

$$g_{ijk}(r) = N x^i y^j z^k e^{-\alpha r^2}. \quad (1.13)$$

1.2.3.1 Minimal basis sets

Minimal basis sets carry the minimum number of basis functions needed for each atom that required permanent size atomic type orbitals. The minimal basis sets is based on STO-3G.

$$\begin{aligned} (2s) &= d_{1s} e^{-1s r^2} + d_{1s} e^{-1s r^2} + d_{1s} e^{-1s r^2} \\ (2p_x) &= d_{1p_x} e^{-1p r^2} + d_{2p_x} e^{-2p r^2} + d_{3p_x} e^{-3p r^2} \\ (2p_y) &= d_{1p_y} e^{-1p r^2} + d_{2p_y} e^{-2p r^2} + d_{3p_y} e^{-3p r^2} \\ (2p_z) &= d_{1p_z} e^{-1p r^2} + d_{2p_z} e^{-2p r^2} + d_{3p_z} e^{-3p r^2} \end{aligned} \quad (1.14)$$

1.2.3.2 Split-valence basis sets

The problem is treating all electrons as equal, therefore split valence basis sets are designed to explain valence orbitals and core orbitals. In split-valence basis sets, the core electrons can be illustrated with a single STO but in fact the valence electron are used more than one contact GTO. The good example of split-valence basis sets is 6-31G basis set, which comprises of 6 gaussians for inner-shell orbital, 3 gaussians for the first STO of valence orbital and 1 gaussian for the second STO.

1.2.3.3 Polarized functions

Polarization functions are extra included in basis sets in trying to simulate the polarization effects model as the atom is closely brought together. Therefore this is a reason of electron cloud shape distortion in the neighborhood atom. The polarized basis sets add D function to carbon atoms and P function to hydrogen atoms to calculate the polarization effect. The polarized basis sets for these function has been detailed in to basic set such as 6-31G(d,p).

1.2.3.4 Effective core potentials

Effective core potential (ECP) has been used for the highly performance in the molecular orbital computing that is appropriate for transition metals. ECP is a category of potential function that could be replaced the inner electrons of atomic and molecular systems and calculate only the valence electrons obviously in quantum molecular computing. The concept was approved the precision of data calculating compared with experimental results and those from an expensive all electron basis sets.

1.2.4 The chemical indices

The chemical indices are obtained by the density calculation. These indices show the specific properties of a chemical species [26].

1.2.4.1 Electronic chemical potential

The chemical potential of the DFT [27], which is variational the principle of equation (1.15), is a very small one-electron energy that is smaller than the total electronic energy. It gets into the variational principle of traditional quantum chemistry.

$$\delta \{ E [n(r)] - \mu [N[n(r)]] \} = 0, \quad (1.15)$$

where μ is a electronic chemical potential, η is a chemical hardness and N is a electron number in molecular system.

It has to solve this equation for every μ , then taking the μ value that makes the correct number of electrons for the system of interest. According to the Lagrangian multipliers, μ determines how sensitive the extreme E is to change in N .

$$\mu = \left(\frac{\partial E}{\partial N} \right)_{r(\bar{r})} \quad (1.16)$$

Approximate of μ can be computed by the equation (1.17) which ionization potential is IP and electron affinity is EA .

$$\mu \approx -\frac{1}{2}(IP + EA) \quad (1.17)$$

1.2.4.2 Mulliken electronegativity

The Milliken electronegativity (χ) [26] is a negative of chemical potential in DFT, shown by equation as:

$$\chi = -\mu. \quad (1.18)$$

1.2.4.3 Chemical hardness

The hardness (η) [28-30] can be described as a resistance to charge transfer. E versus N plot is not straight lines, but is generally convex upward. Their curvatures define another property of substantial importance.

$$\eta = \left(\frac{\partial^2 E}{\partial N^2} \right)_{V(\bar{r})} \quad (1.19)$$

The finite-difference approximation is expressed in equation(1.20). It can be written as

$$\eta \approx -\frac{1}{2}(IP - EA). \quad (1.20)$$

1.2.4.4 Electrophilicity

The electrophilicity (ω) index [31] is used to describe a reliable property of a chemical system and may be used as quantum chemical descriptor. The operational definition is expressed by term of electrophilicity index may be written as

$$\omega = \frac{\mu^2}{2\eta}. \quad (1.21)$$

1.2.4.5 Dipole moment

The asymmetry of a charge distribution is determined by the physical property which is the dipole moment. The dipole moment is shown as the product of the total amount of positive or negative charge and the distance between their centroids. The unit for dipole moments is called a Debye.

1.2.5 Thermodynamic properties

The basic equations used to describe thermochemical quantities [32] such as enthalpy, free energy and rate of reaction.

1.2.5.1 Enthalpies and Gibbs free energies of reaction

The different of the sums of heats of formation is taken to calculate the enthalpies of reaction using this equation

$$\Delta_r H^\circ(298K) = \sum_{prod} \Delta_f H^\circ_{prod}(298K) - \sum_{react} \Delta_f H^\circ_{react}(298K). \quad (1.22)$$

However, there is the way to simply take different of the sums of heats of formation for reactant and the products. Gaussian program provides the short cut to calculate the enthalpy of reaction is defined as

$$\Delta_r H^\circ(298K) = \sum_{prod} (\varepsilon_0 + H_{corr}) - \sum_{react} (\varepsilon_0 + H_{corr}), \quad (1.23)$$

where ε_0 for the total electronic energy. H_{corr} is correction to the enthalpy due to internal energy which can be calculated by

$$H_{corr} = E_{tot} + k_B T, \quad (1.24)$$

where E_{tot} (total internal energy) is the sum of E_t, E_r, E_v, E_e (internal energy due to translation, rotational, vibrational and electronic motion, respectively).

$$E_{tot} = E_t + E_r + E_v + E_e. \quad (1.25)$$

Likewise, Gibbs free energies of reaction can be calculated by the same short cut:

$$\Delta_r G^\circ(298K) = \sum_{prod} (\varepsilon_0 + G_{corr}) - \sum_{react} (\varepsilon_0 + G_{corr}), \quad (1.26)$$

where the correction to the Gibbs free energy due to internal energy (G_{corr}) can be calculated by

$$G_{corr} = H_{corr} - TS_{tot}, \quad (1.27)$$

$$S_{tot} = S_t + S_r + S_v + S_e, \quad (1.28)$$

where S_{tot} (total internal entropy) is the sum of S_t, S_r, S_v, S_e (entropy due to translation, rotational, vibrational and electronic motion, respectively).

1.2.5.2 Rate of reaction

The rate of reaction ($k(T)$) is defined by equation:

$$k(T) = \frac{k_B T}{hc^\circ} e^{-\Delta G^\circ / RT}, \quad (1.29)$$

where k_B is the Boltzmann's constant, h is Plank's constant, T is the absolute temperature, R is the gas constant, $c^\circ = 1$ for the concentration.

1.3 Objective

The adsorptions of diatomic gases (H_2 , N_2 , O_2 , CO , NO), triatomic gases (CO_2 , N_2O , NO_2 , H_2O , H_2S , SO_2), polyatomic gases (C_2H_2 , C_2H_4 , CH_4 , NH_3) on CeO_2 and Ce_2O_4 have been studied. The reduction process of CeO_2 to CeO by H_2 gas have been investigated. Electronic properties and thermodynamic properties of all reactions have been obtained and reported.

CHAPTER II

COMPUTATIONAL DETAILS

2.1 Computational methods

The quantum chemical calculations have been performed with B3LYP method, the Becke's three-parameter hybrid functional [33] combined with the Lee-Yang-Parr correlation functional [34], using Stuttgart RSC ANO/ECP basis set for cerium atom and 6-31G(d) for other atoms. All calculations were performed with the Gaussian 09 program [35].

2.2 Definitions of reaction terms

2.2.1 Adsorption of small gases on cerium oxide

The adsorption energy (ΔE_{ads}) for gas molecules adsorbed on the cerium oxide has been computed by the equation (2.1)

$$\Delta E_{\text{ads}} = E_{\text{gas/cerium oxide}} - (E_{\text{cerium oxide}} + E_{\text{gas}}), \quad (2.1)$$

where $E_{\text{gas/cerium oxide}}$, $E_{\text{cerium oxide}}$ and E_{gas} are total energies of gas adsorption structure on cerium oxide and gas molecule, respectively.

2.2.2 Thermodynamic quantities

The standard enthalpy ΔH_{298} and Gibbs free energy changes ΔG_{298} of adsorption of hydrogen molecule onto CeO_2 have been derived from the frequency calculations at the same level of theory. The equilibrium constant (K) was computed using formula, $\exp(-\Delta G_{298}/RT)$.

CHAPTER III

RESULTS AND DISCUSSIONS

In the present study, adsorptions of diatomic gases (H_2 , N_2 , O_2 , CO , NO), triatomic gases (CO_2 , N_2O , NO_2 , H_2O , H_2S , SO_2) and polyatomic gases (C_2H_2 , C_2H_4 , CH_4 , NH_3) on the CeO_2 and Ce_2O_4 cluster and the reduction reaction of CeO_2 by H_2 gas, were mainly investigated. Therefore, three sections of results are presented.

3.1 The optimized structures

The B3LYP/GEN-optimized structures of CeO_2 and Ce_2O_4 obtained by full geometry optimizations are shown in Figure 3.1.



Figure 3.1 The B3LYP/GEN-optimized structures of (a) CeO_2 and (b) trans- Ce_2O_4 .

3.2 Adsorption of single molecule of gases on the CeO_2 and Ce_2O_4 clusters

3.2.1 Adsorption of gases on the CeO_2

The B3LYP/GEN-optimized structures of adsorption configurations of diatomic gases (H_2 , N_2 , O_2 , CO , NO), triatomic gases (CO_2 , N_2O , NO_2 , H_2O , H_2S , SO_2), polyatomic gases (C_2H_2 , C_2H_4 , CH_4 , NH_3) on CeO_2 are shown in Figure 3.2. It shows that diatomic gases adsorption structure pointing their atom-end toward Ce atom except H_2 whose H-H bond is

perpendicular to Ce atom of CeO₂. The CO₂/CeO₂ adsorption structure, suggests that CO₂ point its oxygen atom toward Ce atom of CeO₂ molecule. The N₂O/CeO₂ adsorption structure has two configurations. One is of pointing its N-end toward Ce atom of CeO₂. O-N bond parallel to Ce-O bond of CeO₂ molecule. Another one is of the pointing its oxygen atom toward Ce atom and nitrogen atom toward oxygen atom. The adsorption structure of NO₂ suggests that N-O bond is approximately perpendicular to Ce atom of CeO₂ structure. The H₂O/CeO₂ adsorption structure suggests that O-H bond of water parallel to Ce-O bond of CeO₂ by pointing its oxygen atom toward Ce atom and hydrogen atom toward O atom of CeO₂ molecule. The adsorption structure of H₂S suggests that their molecular planes are parallel. The adsorption structure of SO₂ suggests, S-O bond is approximately parallel to Ce-O bond by pointing its sulfur atom toward oxygen atom and oxygen atom toward Ce atom. The adsorption structure of triatomic gases suggest that C≡C bond of C₂H₂ and C=C bond of C₂H₄ are perpendicular to Ce atom, CH₄ suggests that its two hydrogen atoms point toward Ce atom and NH₃ suggests that its nitrogen atom point toward Ce atom of CeO₂ molecule.

The energy gaps and chemical indices of CeO₂ and its gas adsorption configurations are shown in Table 3.1. The energy gaps of CeO₂ cluster largely decreased after adsorptions of O₂ and NO gases. The energy gaps of other gases adsorptions with CeO₂ were also not much different from its corresponding bare cluster.

Adsorption abilities of CeO₂ with diatomic, triatomic and polyatomic gases are in orders : O₂($\Delta E_{\text{ads}} = -17.83$ kcal/mol) > NO its N-end toward ($\Delta E_{\text{ads}} = -7.39$ kcal/mol) > CO its C-end toward ($\Delta E_{\text{ads}} = -7.04$ kcal/mol) > CO its O-end toward ($\Delta E_{\text{ads}} = -3.77$ kcal/mol) > NO its O-end toward ($\Delta E_{\text{ads}} = -3.50$ kcal/mol) > N₂ ($\Delta E_{\text{ads}} = -3.30$ kcal/mol) > H₂ ($\Delta E_{\text{ads}} = -1.66$ kcal/mol), H₂O ($\Delta E_{\text{ads}} = -51.45$ kcal/mol) > NO₂ ($\Delta E_{\text{ads}} = -47.91$ kcal/mol) > SO₂ ($\Delta E_{\text{ads}} = -15.85$ kcal/mol) > H₂S ($\Delta E_{\text{ads}} = -7.52$ kcal/mol) > CO₂ ($\Delta E_{\text{ads}} = -5.16$ kcal/mol) > N₂O its O-end toward ($\Delta E_{\text{ads}} = -4.87$ kcal/mol) > N₂O its N-end toward ($\Delta E_{\text{ads}} = -4.26$ kcal/mol) and NH₃ ($\Delta E_{\text{ads}} = -19.62$ kcal/mol) > C₂H₂ ($\Delta E_{\text{ads}} = -10.31$ kcal/mol) > C₂H₄ ($\Delta E_{\text{ads}} = -8.50$ kcal/mol) > CH₄ ($\Delta E_{\text{ads}} = -2.43$ kcal/mol) respectively. Their adsorption energies are shown in Table 3.2.

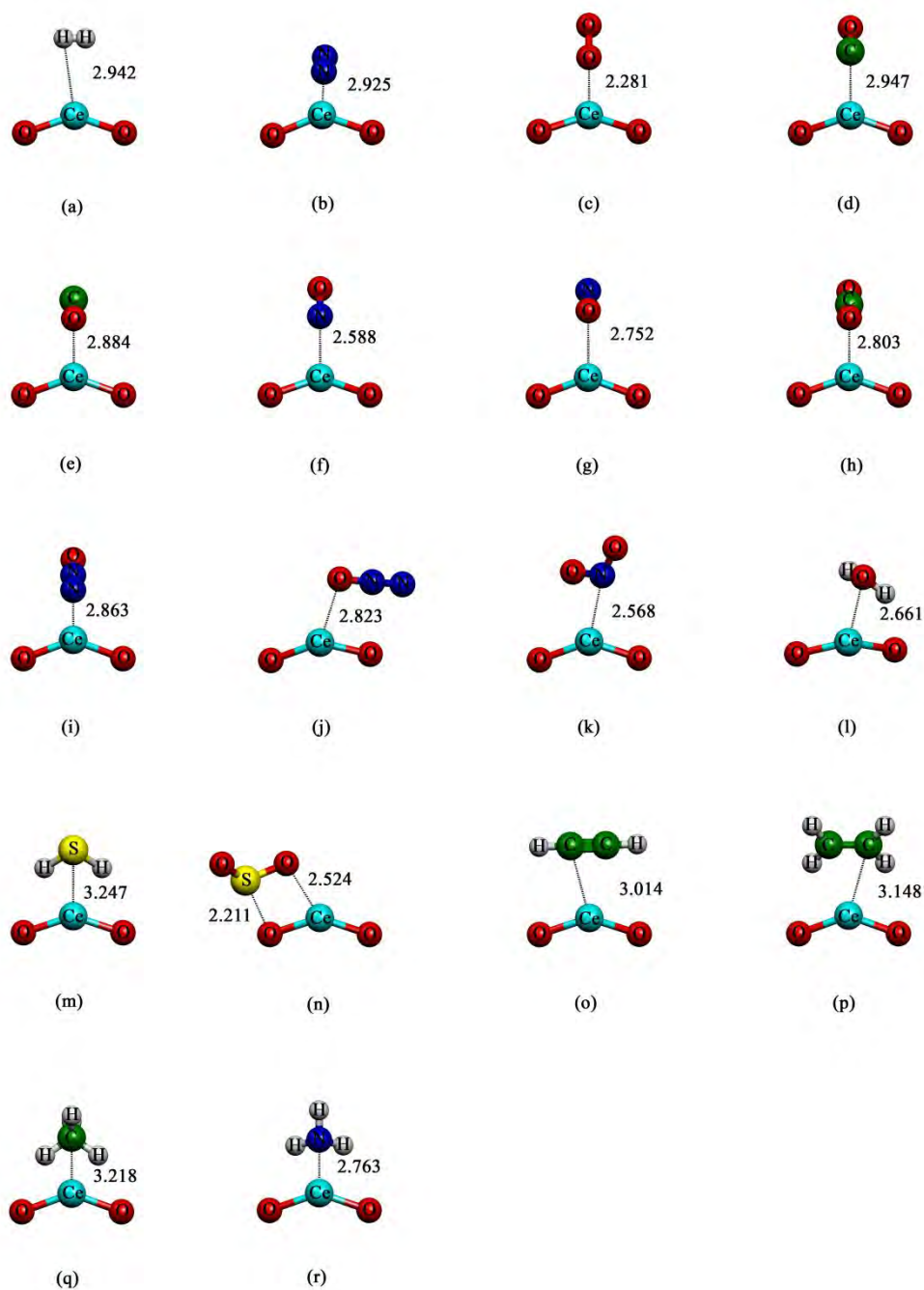


Figure 3.2. The adsorption configurations of (a) H₂, (b) N₂, (c) O₂, (d) CO (its C-end toward), (e) CO (its O-end toward), (f) NO (its N-end toward), (g) NO (its O-end toward), (h) CO₂, (i) N₂O (its N-end toward), (j) N₂O (its O-end toward), (k) NO₂, (l) H₂O, (m) H₂S, (n) SO₂, (o) C₂H₂, (p) C₂H₄, (q) CH₄, (r) NH₃ on CeO₂ cluster, computed at the B3LYP/GEN method. Their bond distances are in Å.

Table 3.1. Energy gap and chemical indices of CeO₂ cluster and its gas adsorptions, computed at the DFT/B3LYP/GEN method.

Compound	$E_{\text{HOMO}}^{\text{a}}$	$E_{\text{LUMO}}^{\text{a}}$	$\Delta E_{\text{gap}}^{\text{a}}$	μ^{b}	χ^{c}	η^{d}	ω^{e}
CeO ₂	-6.006	-1.604	4.402	-3.805	3.805	2.201	3.289
Diatomic							
H ₂ /CeO ₂	-5.962	-1.274	4.688	-3.618	3.618	2.344	2.792
N ₂ /CeO ₂	-5.838	-2.184	3.654	-4.011	4.011	1.827	4.403
O ₂ /CeO ₂	-7.083	-5.121	1.962	-6.102	6.102	0.981	18.976
<u>CO</u> /CeO ₂	-5.806	-2.338	3.468	-4.072	4.072	1.734	4.780
<u>CO</u> /CeO ₂	-5.805	-1.921	3.884	-3.863	3.863	1.942	3.841
<u>NO</u> /CeO ₂	-6.261	-4.178	2.083	-5.220	5.220	1.042	13.079
<u>NO</u> /CeO ₂	-5.968	-4.195	1.773	-5.082	5.082	0.886	14.568
Triatomic							
CO ₂ /CeO ₂	-5.673	-1.216	4.458	-3.444	3.444	2.229	2.661
ON ₂ /CeO ₂	-5.711	-1.978	3.733	-3.845	3.845	1.867	3.959
N ₂ O/CeO ₂	-5.818	-1.362	4.456	-3.590	3.590	2.228	2.893
O ₂ N/CeO ₂	-7.419	-2.699	4.720	-5.059	5.059	2.360	5.423
H ₂ O/CeO ₂	-5.697	-1.177	4.521	-3.437	3.437	2.260	2.613
H ₂ S/CeO ₂	-5.621	-1.142	4.479	-3.382	3.382	2.240	2.553
SO ₂ /CeO ₂	-6.723	-2.799	3.923	-4.761	4.761	1.962	5.777
Polyatomic							
C ₂ H ₂ /CeO ₂	-5.654	-0.998	4.657	-3.326	3.326	2.328	2.376
C ₂ H ₄ /CeO ₂	-5.667	-1.177	4.490	-3.422	3.422	2.245	2.608
CH ₄ /CeO ₂	-5.843	-1.284	4.560	-3.563	3.563	2.280	2.785
H ₃ N/CeO ₂	-5.187	-0.956	4.231	-3.072	3.072	2.116	2.230

compound	$E_{\text{HOMO}a}$	$E_{\text{LUMO}a}$	$\Delta E_{\text{gap}a}$	$\mu\beta$	$\chi\chi$	$\eta\delta$	$\omega\epsilon$
CeO2	-6.006	-1.604	4.402	-3.805	3.805	2.201	3.289
Diatomic							
H2/CeO2	-5.962	-1.274	4.688	-3.618	3.618	2.344	2.792
N2/CeO2	-5.838	-2.184	3.654	-4.011	4.011	1.827	4.403
O2/CeO2	-7.083	-5.121	1.962	-6.102	6.102	0.981	18.976
<u>CO</u> /CeO2	-5.806	-2.338	3.468	-4.072	4.072	1.734	4.780
CO/CeO2	-5.805	-1.921	3.884	-3.863	3.863	1.942	3.841
<u>NO</u> /CeO2	-6.261	-4.178	2.083	-5.220	5.220	1.042	13.079
NO/CeO2	-5.968	-4.195	1.773	-5.082	5.082	0.886	14.568
Triatomic							
CO2/CeO2	-5.673	-1.216	4.458	-3.444	3.444	2.229	2.661
ON2/CeO2	-5.711	-1.978	3.733	-3.845	3.845	1.867	3.959

N2O/CeO2	-5.818	-1.362	4.456	-3.590	3.590	2.228	2.893
O2N/CeO2	-7.419	-2.699	4.720	-5.059	5.059	2.360	5.423
H2O/CeO2	-5.697	-1.177	4.521	-3.437	3.437	2.260	2.613
H2S/CeO2	-5.621	-1.142	4.479	-3.382	3.382	2.240	2.553
SO2/CeO2	-6.723	-2.799	3.923	-4.761	4.761	1.962	5.777
Polyatomic							
C2H2/CeO2	-5.654	-0.998	4.657	-3.326	3.326	2.328	2.376

^a In eV.

^b Electronic chemical potential, $\mu = (E_{\text{HOMO}} + E_{\text{LUMO}})/2$

^c The Mulliken electronegativity index, $\chi = -(E_{\text{HOMO}} + E_{\text{LUMO}})/2$

^d Chemical hardness, $\eta = (E_{\text{LUMO}} - E_{\text{HOMO}})/2$, $\eta = E_{\text{gap}}/2$

^e The electrophilicity index, $\omega = \mu^2/2\eta$



Table 3.2 Adsorption energies of diatomic, triatomic and polyatomic gases on the CeO₂ cluster, computed at the B3LYP/GEN method.

Gases adsorption				Δ_{ads}^a	
Diatomic					
CeO ₂	+	H ₂	→	H ₂ /CeO ₂	-1.66
CeO ₂	+	N ₂	→	N ₂ /CeO ₂	-3.30
CeO ₂	+	O ₂	→	O ₂ /CeO ₂	-17.83
CeO ₂	+	CO	→	<u>CO</u> /CeO ₂	-7.04
CeO ₂	+	CO	→	<u>CQ</u> /CeO ₂	-3.77
CeO ₂	+	NO	→	<u>NO</u> /CeO ₂	-7.39
CeO ₂	+	NO	→	<u>NO</u> /CeO ₂	-3.50
Triatomic					
CeO ₂	+	CO ₂	→	CO ₂ /CeO ₂	-5.16
CeO ₂	+	N ₂ O	→	<u>ON</u> ₂ /CeO ₂	-4.26
CeO ₂	+	N ₂ O	→	N ₂ <u>O</u> /CeO ₂	-4.87
CeO ₂	+	NO ₂	→	O ₂ <u>N</u> /CeO ₂	-47.91
CeO ₂	+	H ₂ O	→	H ₂ O/CeO ₂	-51.45
CeO ₂	+	H ₂ S	→	H ₂ S/CeO ₂	-7.52
CeO ₂	+	SO ₂	→	SO ₂ /CeO ₂	-15.85
Polyatomic					
CeO ₂	+	C ₂ H ₂	→	C ₂ H ₂ /CeO ₂	-10.31
CeO ₂	+	C ₂ H ₄	→	C ₂ H ₄ /CeO ₂	-8.50
CeO ₂	+	CH ₄	→	CH ₄ /CeO ₂	-2.43
CeO ₂	+	NH ₃	→	H ₃ N/CeO ₂	-19.62

^a In kcal/mol.

ภาควิชาเคมี
คณะวิทยาศาสตร์
จุฬาลงกรณ์มหาวิทยาลัย

3.2.2 Adsorption of gases on Ce₂O₄

The B3LYP/GEN-optimized structures of adsorption configurations of diatomic gases (H₂, N₂, O₂, CO, NO), triatomic gases (CO₂, N₂O, NO₂, H₂O, H₂S, SO₂), polyatomic gases (C₂H₂, C₂H₄, CH₄, NH₃) on Ce₂O₄ are shown in Figure 3.3. The H₂/Ce₂O₄ adsorption structure suggests that H-H bond is perpendicular to Ce atom of Ce₂O₄. The adsorption structure of N₂ suggests that its nitrogen atom point toward Ce atom of Ce₂O₄. The O₂/Ce₂O₄ adsorption structure suggests that O-O bond is perpendicular to Ce atom of Ce₂O₄. The CO/Ce₂O₄ adsorption structure suggests that pointing atom-end toward Ce atom of Ce₂O₄. The NO/Ce₂O₄ adsorption structure has two configurations. One is of the pointing its N-end toward Ce atom of Ce₂O₄. Another one is of the N-O bond is perpendicular to Ce atom of Ce₂O₄. The adsorption structure of CO₂ suggests that pointing oxygen atom toward Ce atom of Ce₂O₄. The N₂O/Ce₂O₄ adsorption structure suggests that has two configurations. One is of the pointing its N-end toward Ce atom of Ce₂O₄. Another one is of the O-N bond parallel to Ce-O bond of Ce₂O₄ molecule by pointing its oxygen atom toward Ce atom and nitrogen atom toward oxygen atom. The NO₂/Ce₂O₄ adsorption structure suggests that N-O bond is approximately parallel to Ce-O bond of Ce₂O₄ molecule by pointing its oxygen atom toward Ce atom and nitrogen atom toward Ce atom. The adsorption structure of water suggests that its oxygen atom point toward Ce atom. The H₂S/Ce₂O₄ adsorption structure suggests that its hydrogen atom point toward oxygen atom of Ce₂O₄. The SO₂/Ce₂O₄ adsorption structure suggests that S=O bond is parallel to Ce-O bond of Ce₂O₄ by pointing its oxygen atom toward Ce atom and sulfur atom toward oxygen atom. The adsorption structure of triatomic gases suggest that C≡C bond of C₂H₂ and C=C bond of C₂H₄ are perpendicular to Ce atom, CH₄ suggests that its two hydrogen atoms point toward Ce atom and NH₃ suggests that its nitrogen atom point toward Ce atom of Ce₂O₄ molecule.

The energy gaps and chemical indices of Ce₂O₄ and its gas adsorption configurations are shown in Table 3.3. The energy gaps of Ce₂O₄ cluster largely decreased after adsorptions of O₂ and NO gases. The energy gaps of other gases adsorptions with Ce₂O₄ were also not much different from its corresponding bare cluster.

Adsorption abilities of Ce₂O₄ with diatomic, triatomic and polyatomic gases are in orders: O₂($\Delta E_{\text{ads}} = -8.52$ kcal/mol) > CO its C-end toward ($\Delta E_{\text{ads}} = -6.19$ kcal/mol) > NO its N-end toward ($\Delta E_{\text{ads}} = -3.93$ kcal/mol) > CO its O-end toward ($\Delta E_{\text{ads}} = -3.40$ kcal/mol) > N₂ ($\Delta E_{\text{ads}} = -2.67$ kcal/mol) > NO its O-end toward ($\Delta E_{\text{ads}} = -2.29$ kcal/mol) > H₂ ($\Delta E_{\text{ads}} = -1.13$

kcal/mol), H₂O ($\Delta E_{\text{ads}} = -52.45$ kcal/mol) > NO₂ ($\Delta E_{\text{ads}} = -42.02$ kcal/mol) > SO₂ ($\Delta E_{\text{ads}} = -13.87$ kcal/mol) > H₂S ($\Delta E_{\text{ads}} = -7.14$ kcal/mol) > CO₂ ($\Delta E_{\text{ads}} = -4.85$ kcal/mol) > N₂O its O-end toward ($\Delta E_{\text{ads}} = -4.32$ kcal/mol) > N₂O its N-end toward ($\Delta E_{\text{ads}} = -3.71$ kcal/mol) and NH₃ ($\Delta E_{\text{ads}} = -19.65$ kcal/mol) > C₂H₂ ($\Delta E_{\text{ads}} = -8.66$ kcal/mol) > C₂H₄ ($\Delta E_{\text{ads}} = -7.94$ kcal/mol) > CH₄ ($\Delta E_{\text{ads}} = -2.13$ kcal/mol) respectively. Their adsorption energies are shown in Table 3.4.



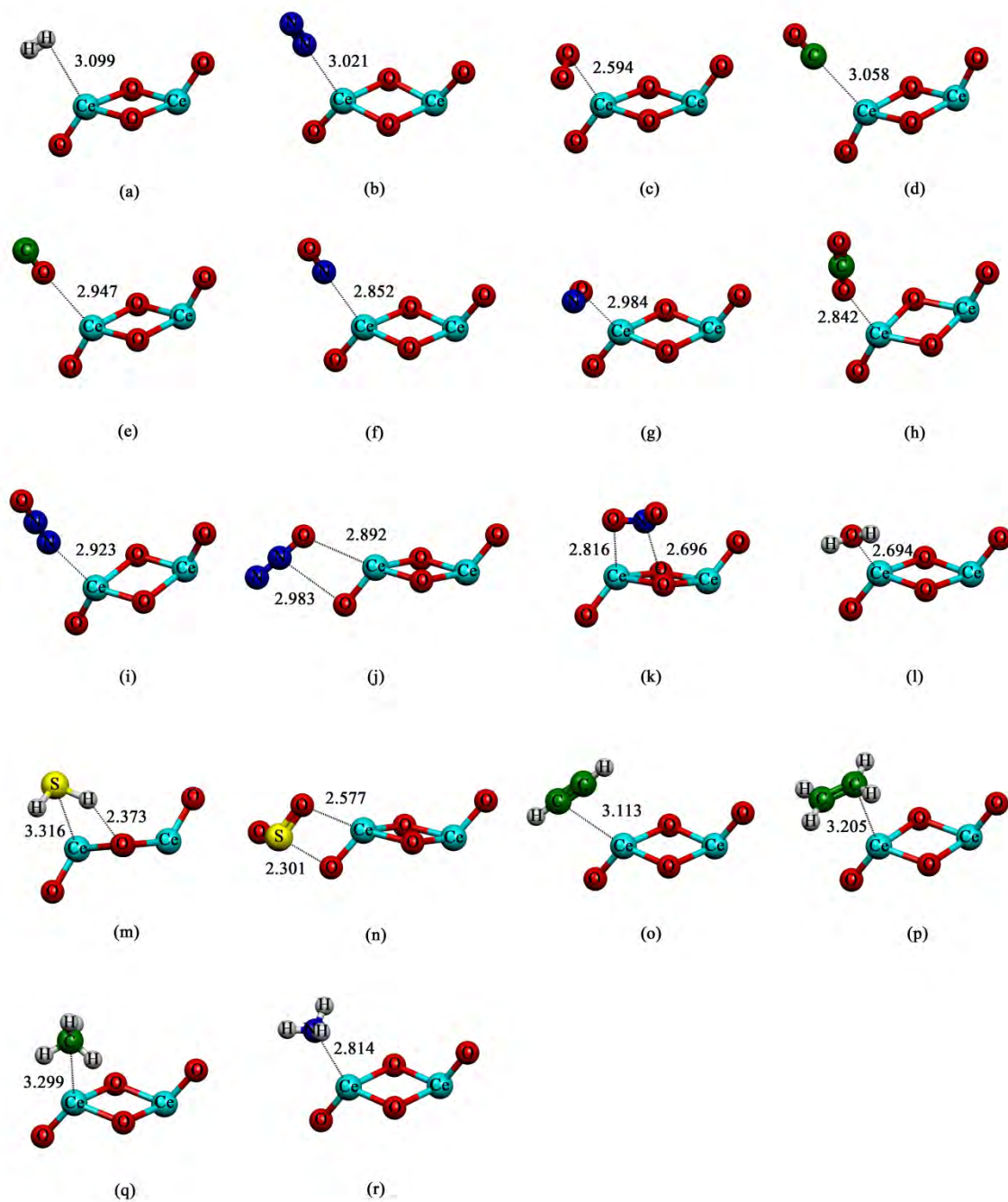


Figure 3.3. The adsorption configurations of (a) H₂, (b) N₂, (c) O₂, (d) CO (its C-end toward), (e) CO (its O-end toward), (f) NO (its N-end toward), (g) NO (its O-end toward), (h) CO₂, (i) N₂O (its N-end toward), (j) N₂O (its O-end toward), (k) NO₂, (l) H₂O, (m) H₂S, (n) SO₂, (o) C₂H₂, (p) C₂H₄, (q) CH₄, (r) NH₃ on Ce₂O₄ cluster, computed at the B3LYP/GEN method. Their bond distances are in Å.

Table 3.3. Energy gap and chemical indices of Ce₂O₄ cluster and its gas adsorption on the Ce₂O₄ cluster, computed at the DFT/B3LYP/GEN method.

compound	$E_{\text{HOMO}}^{\text{a}}$	$E_{\text{LUMO}}^{\text{a}}$	$\Delta E_{\text{gap}}^{\text{a}}$	μ^{b}	χ^{c}	η^{d}	ω^{e}
Ce ₂ O ₄	-6.744	-2.032	4.713	-4.388	4.388	2.356	4.086
Diatomic							
H ₂ /Ce ₂ O ₄	-6.706	-1.992	4.715	-4.349	4.349	2.357	4.012
N ₂ /Ce ₂ O ₄	-6.604	-2.338	4.267	-4.471	4.471	2.133	4.685
O ₂ /Ce ₂ O ₄	-7.001	-5.938	1.063	-6.470	6.470	0.531	39.379
<u>C</u> O/Ce ₂ O ₄	-6.573	-2.488	4.085	-4.530	4.530	2.043	5.024
<u>C</u> <u>O</u> /Ce ₂ O ₄	-6.594	-2.101	4.493	-4.347	4.347	2.247	4.206
<u>N</u> O/Ce ₂ O ₄	-6.643	-4.490	2.152	-5.566	5.566	1.076	14.395
<u>N</u> <u>O</u> /Ce ₂ O ₄	-6.634	-4.261	2.373	-5.448	5.448	1.187	12.503
Triatomic							
CO ₂ /Ce ₂ O ₄	-6.509	-1.832	4.677	-4.170	4.170	2.338	3.719
ON ₂ /Ce ₂ O ₄	-6.514	-2.131	4.383	-4.322	4.322	2.192	4.262
N ₂ O/Ce ₂ O ₄	-6.625	-1.913	4.712	-4.269	4.269	2.356	3.867
O ₂ N/Ce ₂ O ₄	-6.777	-3.020	3.757	-4.899	4.899	1.878	6.388
H ₂ O/Ce ₂ O ₄	-6.292	-1.656	4.635	-3.974	3.974	2.318	3.407
H ₂ S/Ce ₂ O ₄	-6.646	-1.969	4.677	-4.307	4.307	2.339	3.966
SO ₂ /Ce ₂ O ₄	-7.060	-3.066	3.994	-5.063	5.063	1.997	6.417
Polyatomic							
C ₂ H ₂ /Ce ₂ O ₄	-6.482	-1.782	4.700	-4.132	4.132	2.350	3.633
C ₂ H ₄ /Ce ₂ O ₄	-6.478	-1.826	4.652	-4.152	4.152	2.326	3.706
CH ₄ /Ce ₂ O ₄	-6.644	-1.935	4.709	-4.289	4.289	2.355	3.906
H ₃ N/Ce ₂ O ₄	-6.146	-1.550	4.596	-3.848	3.848	2.298	3.221

^a In eV.

^b Electronic chemical potential, $\mu = (E_{\text{HOMO}} + E_{\text{LUMO}})/2$

^c The Mulliken electronegativity index, $\chi = -(E_{\text{HOMO}} + E_{\text{LUMO}})/2$

^d Chemical hardness, $\eta = (E_{\text{LUMO}} - E_{\text{HOMO}})/2$, $\eta = E_{\text{gap}}/2$

^e The electrophilicity index, $\omega = \mu^2/2\eta$

Table 3.4. Adsorption energies of diatomic, triatomic and polyatomic gases on the Ce₂O₄ cluster, computed at the B3LYP/GEN method.

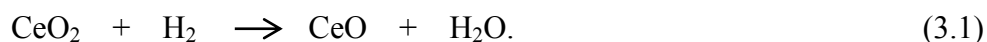
Gases adsorption				$\Delta_{\text{ads}}^{\text{a}}$	
Diatomic					
Ce ₂ O ₄	+	H ₂	→	H ₂ /Ce ₂ O ₄	-1.13
Ce ₂ O ₄	+	N ₂	→	N ₂ /Ce ₂ O ₄	-2.67
Ce ₂ O ₄	+	O ₂	→	O ₂ /Ce ₂ O ₄	-8.52
Ce ₂ O ₄	+	CO	→	<u>C</u> O/Ce ₂ O ₄	-6.19
Ce ₂ O ₄	+	CO	→	C <u>O</u> /Ce ₂ O ₄	-3.40
Ce ₂ O ₄	+	NO	→	<u>N</u> O/Ce ₂ O ₄	-3.93
Ce ₂ O ₄	+	NO	→	N <u>O</u> /Ce ₂ O ₄	-2.29
Triatomic					
Ce ₂ O ₄	+	CO ₂	→	CO ₂ /Ce ₂ O ₄	-4.85
Ce ₂ O ₄	+	N ₂ O	→	<u>O</u> N ₂ /Ce ₂ O ₄	-3.71
Ce ₂ O ₄	+	N ₂ O	→	N ₂ <u>O</u> /Ce ₂ O ₄	-4.32
Ce ₂ O ₄	+	NO ₂	→	O ₂ <u>N</u> /Ce ₂ O ₄	-42.02
Ce ₂ O ₄	+	H ₂ O	→	H ₂ O/Ce ₂ O ₄	-52.45
Ce ₂ O ₄	+	H ₂ S	→	H ₂ S/Ce ₂ O ₄	-7.14
Ce ₂ O ₄	+	SO ₂	→	SO ₂ /Ce ₂ O ₄	-13.87
Polyatomic					
Ce ₂ O ₄	+	C ₂ H ₂	→	C ₂ H ₂ /Ce ₂ O ₄	-8.66
Ce ₂ O ₄	+	C ₂ H ₄	→	C ₂ H ₄ /Ce ₂ O ₄	-7.94
Ce ₂ O ₄	+	CH ₄	→	CH ₄ /Ce ₂ O ₄	-2.13
Ce ₂ O ₄	+	NH ₃	→	H ₃ N/Ce ₂ O ₄	-19.65

^a In kcal/mol.

ภาควิชาเคมี
คณะวิทยาศาสตร์
จุฬาลงกรณ์มหาวิทยาลัย

3.3 The reduction of CeO₂ to CeO by H₂ gas.

The reaction considered for H₂ interacting with CeO₂ is the water elimination:



This reaction is accompanied by the reduction of the cerium site from formal oxidation state Ce⁺⁴ (f⁰) to Ce⁺² (f²). The B3LYP/GEN-optimized structures of CeO₂, CeO and the related intermediates and transition states are displayed in Figure 3.4. The first step in the reaction is the formation of a H₂/CeO₂ compound 1, followed by the addition of H₂ to the Ce–O bond forming a OCe(H)OH intermediate 2. Next, two paths for the formation of a H₂O/CeO compound 4 are considered: the concerted pathway of water from OCe(H)OH, or the stepwise pathway by the migration of one hydrogen forming the Ce(OH)₂ intermediate 3. The final step is the elimination of water in the H₂O/CeO compound 4. Potential energy profile for reduction of CeO₂ to CeO by H₂ gas is also shown in Figure 3.5. It obviously shows that CeO₂ is more energetic preferred than CeO. Energies, thermodynamic properties, rate constants, and equilibrium constants of reduction reaction are shown in Table 3.5. The rate determining steps for the Stepwise pathway and Concerted pathway are 1.02×10^{-18} and $2.73 \times 10^{-23} \text{ s}^{-1}$, respectively. The overall equilibrium constants for the Stepwise pathway and Concerted pathway are 3.30×10^{-163} and 2.66×10^{-31} , respectively. The overall reaction enthalpies of both pathways are endothermic process. The Gibbs free energy of the reaction is 234.1 kcal/mol. It was found that the CeO₂ reduced to the CeO cluster by H₂ gas is non-spontaneous reaction at 298 K.

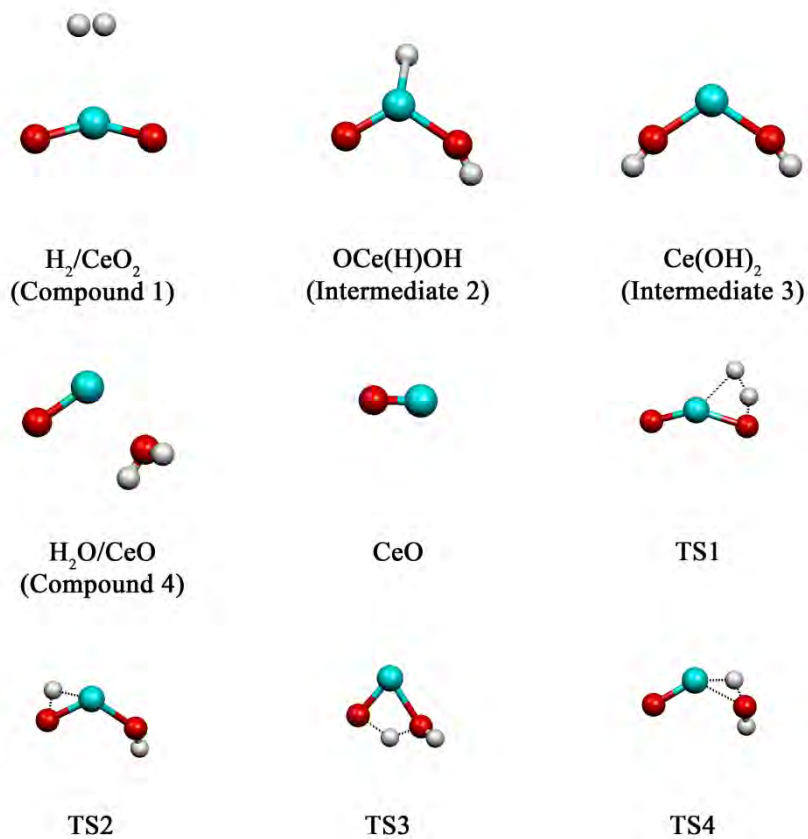


Figure 3.4 B3LYP/GEN-optimized structures of CeO_2 , CeO and the related intermediates and transition states.

Table 3.5 Energetics, thermodynamic properties, rate constants, and equilibrium constants of reduction reaction of CeO₂ to CeO, computed at the DFT/B3LYP/GEN method.

Reaction	$\Delta E^{\ddagger a}$	$\Delta G^{\ddagger a}$	k_{298}^b	ΔE^a	ΔH_{298}^a	ΔG_{298}^a	K_{298}
CeO ₂ + H ₂ → H ₂ /CeO ₂	–	–	–	-0.23	-0.50	4.08	1.03×10 ⁻³
H ₂ /CeO ₂ → TS1 → OCe(H)OH	22.06	20.72	3.83×10 ⁻⁵	6.60	5.80	8.36	7.43×10 ⁻⁷
<i>Stepwise pathway</i>							
OCe(H)OH → TS2 → Ce(OH) ₂	42.47	42.18	1.02×10 ⁻¹⁸	16.73	16.61	16.84	4.55×10 ⁻¹³
Ce(OH) ₂ → TS3 → H ₂ O/CeO	35.81	36.46	3.19×10 ⁻¹⁴	25.48	25.58	24.87	5.85×10 ⁻¹⁹
H ₂ O/CeO → CeO + H ₂ O	–	–	–	185.86	186.03	179.94	1.24×10 ⁻¹³²
<i>Concerted pathway</i>							
OCe(H)–OH → TS4 → H ₂ O/CeO	48.61	48.15	2.73×10 ⁻²³	42.20	42.19	41.71	2.66×10 ⁻³¹

^a In kcal/mol.

^b In s⁻¹.

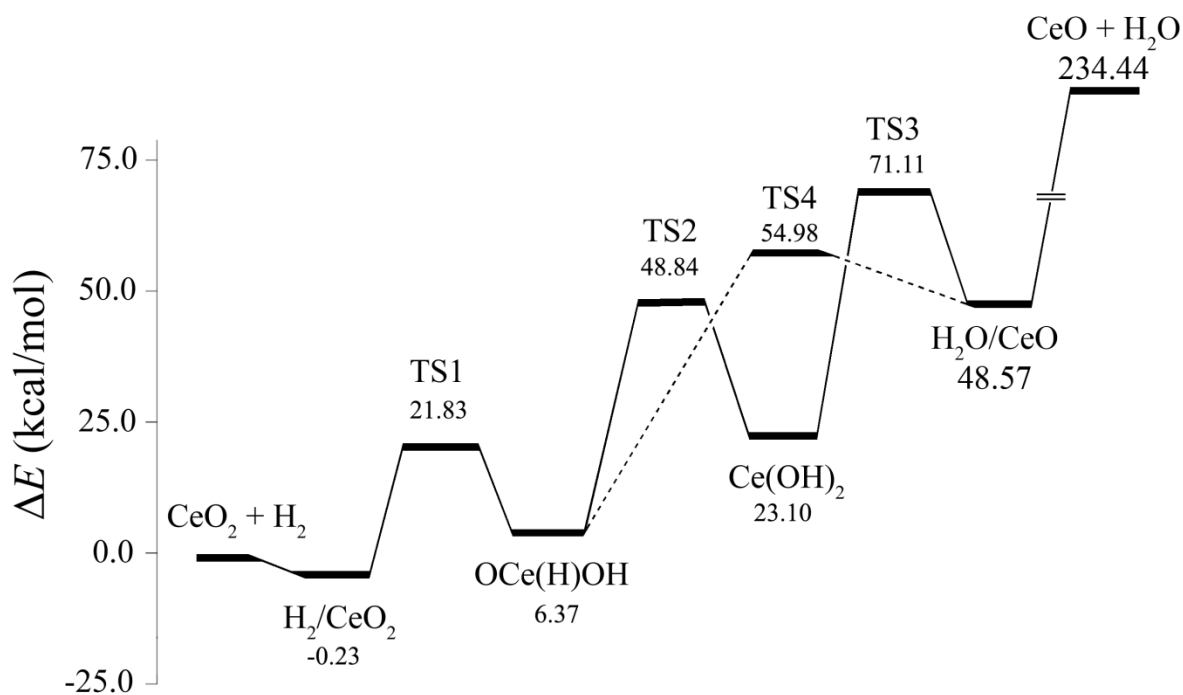


Figure 3.5. Potential energy profile for reduction of CeO₂ to CeO by hydrogen gas.

CHAPTER IV

CONCLUSIONS

A theoretical study on the adsorption of diatomic gases, triatomic gases and polyatomic gases on the CeO_2 and Ce_2O_4 clusters for all possible configurations were investigated at the B3LYP/GEN level of theory. All the results can be concluded as follows:

1. The adsorption of various gases on CeO_2 and Ce_2O_4 is physisorption.
2. The energy gaps of CeO_2 and Ce_2O_4 are largely reduced after the adsorptions of O_2 and NO on CeO_2 and Ce_2O_4 .
3. The CeO_2 and Ce_2O_4 are sensitive material for O_2 and NO . they could be developed as sensor based on electrical conductivity.

The reaction process of the CeO_2 reduced to the CeO cluster by H_2 gas was investigated at the B3LYP/GEN level of theory. It was found that the reduction reaction of CeO_2 to CeO by H_2 gas consist of two pathways. The first pathway is the conversion of OCe(H)OH to Ce(OH)_2 before to $\text{H}_2\text{O/CeO}$ and the second one is the conversion to $\text{H}_2\text{O/CeO}$. The overall equilibrium constants for the Stepwise pathway and Concerted pathway are 3.30×10^{-163} and 2.66×10^{-31} , respectively. The overall reaction enthalpies of both pathways are endothermic process. It was found that the CeO_2 reduced to the CeO cluster by H_2 gas is non-spontaneous reaction at 298 K.

ภาควิชาเคมี
คณะวิทยาศาสตร์
จุฬาลงกรณ์มหาวิทยาลัย

REFERENCES

- [1] Tsunekawa S., Sahara R., Kawazoe Y., Kasuya A., A Origin of the blue shift in ultraviolet absorption spectra of nanocrystalline CeO_{2-x} particles. *Mater. Trans. JIM.* **2000**, *41*, 1104–1107.
- [2] Trovarelli A., de Leitenburg C., Boaro M., Dolcetti G., The utilization of ceria in industrial catalysis, *Catal. Today.* **1999**, *50*, 353–367.
- [3] Zhou F., Zhao X., Xu H., Yuan C., CeO₂ spherical crystallites: synthesis, formation mechanism, size control, and electrochemical property study, *J. Phys. Chem. C.* **2007**, *111*, 1651–1657.
- [4] Chen H., Chang H., Synthesis and characterization of nanocrystalline cerium oxide powders by two-stage non-isothermal precipitation, *Solid State Commun.* **2005**, *133*, 593–598.
- [5] Shahin A., Grandjean F., Long J., Schuman T., Cerium L₃-edge XAS investigation of the structure of crystalline and amorphous cerium oxides, *Chem. Mater.* **2005**, *17*, 315–321.
- [6] Trovarelli A., Catalytic Properties of Ceria and CeO₂-Containing Materials, *Catal. Rev. Sci. En.* **1996**, *38*, 439.
- [7] Kaspar J., Fornasiero P., Graziani M., Use of CeO₂-based oxides in the three-way catalysis, *Catal. Today.* **1999**, *50*, 285.
- [8] Rodrigue Z., Wang X., Hanson J.C., Liu G., Iglesias-Juez A., FernándezGarcía M., The Behavior of Mixed-Metal Oxides: Structural and Electronic Properties of Ce_{1-x}Ca_xO₂ and Ce_{1-x}Ca_xO_{2-x}, *J. Chem. Phys.* **2003**, *119*, 5659.
- [9] Taylor K., Nitric oxide catalysis in automotive exhaust systems. *Catal. Rev. Sci. Eng.* **1995**, *35*, 457.
- [10] Eisenberger P., Basic Research Needs for Vehicles of the Future, Princeton Materials Institute, Princeton, NJ, **1995**.
- [11] Murray E., Tsai T., Barnett S., A direct methane fuel cell with a ceria based a node. *Nature.* **1999**, *400*, 649–651.

- [12] Corma A., Atienzar P., Garcia H., Chane-Ching J.Y., Hierarchically mesostructured doped CeO₂ with potential for solar-cell use. *Nat. Mater.* **2004**, *3*, 394–397.
- [13] Izu, N., Shin, W., Matsubara, I., Murayama, N., Development of resistive oxygen sensors based on cerium oxide thick film. *J. Electroceram.* **2004**, *13*, 703–706.
- [14] Zheng X., Zhang X., Wang, X., Wang S., Wu S., Preparation and characterization of CuO/CeO₂ catalysts and their applications in low-temperature CO oxidation. *Appl. Catal. A: Gen.* **2005**, *295*, 142–149.
- [15] Chen H. L., Weng M. H., Ju S. P., Chang J. G., Chen H. T., Chang C. S., Structural and electronic properties of Ce_nO_{2n} (n = 1–5) nanoparticles: A computational study. *Molecu. Struc.* **2010**, *963*, 2–8.
- [16] Syzgantseva O., Calatayud M., Minot C. Theoretical study of H₂ dissociation on a ZrO₂ cluster. *Chem. Phys. Letters.* **2011**, *503*, 12–17.
- [17] P. Flukiger, H.P. Luthi, S. Portmann, J. Weber, MOLEKEL 4.3, Swiss Center for Scientific Computing, Manno, Switzerland, 2000.
- [18] Levine, N. Quantum chemistry. 6th Ed. Pearson prentice hall, 2010.
- [19] Young, D. C. Computational chemistry, John Wiley and Sons, New York, 2001.
- [20] Engel, T.; Reid, P. Physical chemistry. Pearson Benjamin chummings, 2009.
- [21] Sousa, S. F.; Fernandes, P. A.; Ramos M. J. *J. Phys. Chem. A.* **2007**, *111*, 10439.
- [22] Becke, A. D. Density-Functional Thermochemistry. III. The role of exact exchange, *J. Chem. Phys.* **1993**, *98*, 564 - 5652.
- [23] Ochterski, J.W. Thermochemistry in Gaussian. Gaussian Inc., Pittsburgh 2000.
- [24] Leszczynski, J. Handbook of Computational Chemistry, Springer, New York, 2012.
- [25] Lewars, E. G. Introduction to the theory and applications of molecular and quantum mechanics, 2nd Ed., Springer, Canada, 2003.
- [26] W. Kohn, A.D. Becke, R.G Parr, *Density functional theory of electronic structure.* *J. Phys Chem.* **1996**, *100*, 12974-12980.

- [27] R.G. Parr, R.A. Donnelly, M. Levy, W.E. Palke, Electronegativity: The density functional view point. *J. Chem. Phys.*, 1978. **68**: p. 3801.
- [28] Parr, R.G. and R.G. Pearson, Absolute hardness: comparison parameter to absolute electronegativity. *J. Am. Chem. Soc.*, 1983. **105**: p. 7512.
- [29] W. Yang, R.G. Parr, Hardness, softness, and Fukui function in the electronic theory of metal and catalysis. *Proc. Natl. Acad. Sci* 1985. **82**: p. 6723.
- [30] F.A. Parr, H.K. Srivastana, Y. Beg, P.P. Singh, DFT Based Electrophilicity Index and QSAR study of Phenols as Anti Leukaemia Agent. 2006. **21**: p. 23-28.
- [31] R.G. Parr, L.v. Szentpaly, S. Liu, *Electrophilicity Index*. *J. Am. Chem. Soc.*, 1999. **121**: p. 1922.
- [32] J. Ochterski, *Thermochemistry in Gaussian*. Gaussian, Inc., 2000.
- [33] Lee, C.; Yang, W.; Parr, R.G. *Phys. Rev. B*. **1988**, 37, 785.
- [34] Leang, S. S.; Zahariev, F.; Gordon, M. S.; *J. Chem. Phys.* **1993**, 98, 5648.
- [35] Frisch, M. J.; Trucks, G. W.; Schlegel, H. B.; Scuseria, G. E.; Robb, M. A.; Cheeseman, J. R.; Scalmani, G.; Barone, V.; Mennucci, B.; Petersson, G. A.; Nakatsuji, H.; Caricato, M.; Li, X.; Hratchian, H. P.; Izmaylov, A. F.; Bloino, J.; Zheng, G.; Sonnenberg, J. L.; Hada, M.; Ehara, M.; Toyota, K.; Fukuda, R.; Hasegawa, J.; Ishida, M.; Nakajima, T.; Honda, Y.; Kitao, O.; Nakai, H.; Vreven, T.; Montgomery Jr., J. A.; J. E. Peralta, J. E.; Ogliaro, F.; Bearpark, M.; Heyd, J. J.; Brothers, E.; Kudin, K. N.; Staroverov, V. N.; Keith, T.; Kobayashi, R.; Normand, J.; Raghavachari, K.; Rendell, A.; Burant, J. C.; Iyengar, S. S.; Tomasi, J.; Cossi, M.; Rega, N.; Millam, J. M.; Klene, M.; Knox, J. E.; Cross, J. B.; Bakken, V.; Adamo, C.; Jaramillo, J.; Gomperts, R.; Stratmann, R. E.; Yazyev, O.; Austin, A. J.; Cammi, R.; Pomelli, C.; Ochterski, J. W.; Martin, R. L.; Morokuma, K.; Zakrzewski, V. G.; Voth, G. A.; Salvador, P.; Dannenberg, J. J.; Dapprich, S.; Daniels, A. D.; Farkas, O.; Foresman, J. B.; Ortiz, J. V.; Cioslowski, J.; Fox, D. J. *Gaussian 09, Revision B.01*, Gaussian, Inc., Wallingford CT, 2010.

VITAE

My name is Pattanarak Swing. I was born on 6th July, 1992. My address is 82 M. 14, T. Pa Maet, A. Muang Phrae, Phrae province 54000. My contact is 081-9488486 (Tel.) and pattanarak.p@hotmail.com. I studied primary school at Maradaupathum School during 1999-2004. I studied high school at Piriyalai School Phrae during 2005-2010. I studied Bachelor's degree of Science, Chulalongkorn University during 2011-2014.

